Microporous and Mesoporous Materials 230 (2016) 208–216

Contents lists available at ScienceDirect

Microporous and Mesoporous Materials

journal homepage: www.elsevier.com/locate/micromeso

Synthesis of chabazite/polymer composite membrane for CO_2/N_2 separation

Chenhu Sun, Deepansh J. Srivastava, Philip J. Grandinetti, Prabir K. Dutta*

Department of Chemistry and Biochemistry, The Ohio State University, Columbus, OH, 43210, USA

ARTICLE INFO

Article history:
Received 17 February 2016
Received in revised form
24 April 2016
Accepted 27 April 2016
Available online 6 May 2016

Keywords:
Interzeolite conversion
Faujasite
Raman
Solid state silicon NMR
Nano chabazite

ABSTRACT

There is considerable interest in using zeolite membranes for gas separations. For CO_2 and N_2 separation, much research has focused on faujasitic (FAU) membranes. Simulations suggest that chabazite (CHA) membranes can also be good at CO_2 and N_2 separation. In this study, we have focused on CHA membranes grown on porous polymeric polyethersulfone (PES) supports. Recently, we have reported on a dehydration rehydration hydrothermal (DRHT) process for FAU membrane growth on PES supports, which results in rapid crystallization. It is well known that FAU can be converted to CHA by an interzeolite conversion method, and is our choice for CHA synthesis in this study. A synthesis method for isolated CHA nanocrystals with size of 50–100 nm is reported. Rapid DRHT-based CHA powder synthesis and CHA/PES membrane growth are also being reported, all made by the interzeolite conversion of FAU. The CHA/PES membranes of ~4 μm thickness were coated with polydimethylsiloxane (PDMS), and at 25 °C, CO_2 permeance of 1243 GPU with CO_2/N_2 selectivity of 19 was observed. The porosity of the PES support was critical to enhancing the formation and stability of the CHA membrane, since the CHA membrane on the PES surface was bonded to interconnected CHA crystals that grew within the PES from the seed crystals.

© 2016 Elsevier Inc. All rights reserved.

1. Introduction

Global climate changes has spurred the development of several strategies to reduce atmospheric CO_2. One of the possibilities being explored is to capture CO_2 from large stationary sources such as coal burning power plants and dispose of it in deep wells [1,2]. There are several competing technologies for CO_2 capture including solvent absorption, chemical and physical adsorption, and membranes processes [3]. Polymer membranes, in particular, have shown promise for separating CO_2 from N_2 in post-combustion processes, though commercial application of such technologies have not yet been realized [4]. Another class of membranes based on inorganic aluminosilicate microporous zeolites can also separate gas mixtures on the basis of differences in the molecular size and shape, as well as different adsorption properties [5–7].

Many types of zeolite membranes have been studied, with commercial application limited to zeolite A membranes for solvent dehydration by pervaporation [8]. There are no industrial applications reported yet for zeolite membranes for gas separation [9]. One of the reasons for this is that zeolite membrane modules are considerably more expensive than polymer membranes. Yet, the stability of inorganic membranes, as well as their potentially high flux and gas separation characteristics are attractive and thus, there is considerable ongoing research in this area.

Faujasite (FAU) membranes have been synthesized and tested for the separation of CO_2 from gas streams [10,11]. Chabazite (CHA), another zeolite has potential for the capture and removal of CO_2 from gas mixtures. The building-units of chabazite are the double 6-membered ring (D6R) with a large ellipsoidal cavity (7.3 Å × 12 Å) accessible by six 8-membered ring windows (free aperture ~ 3.8 Å) [12]. It has been reported that among many kinds of naturally occurring and synthetic zeolites, chabazite (CHA) and 13× (FAU) are most suitable for CO_2 separation by pressure swing adsorption techniques [13]. In another study covering adsorption-based CO_2 capture, it was found that CHA held comparative advantages for high temperature CO_2 separation while FAU zeolites showed superior performance at relatively low temperatures [14]. The permeation selectivity of CO_2 over N_2 in CHA zeolite membranes is estimated to be as high as ~20–30, indicating that CHA zeolites can

* Corresponding author.
E-mail address: dutta.1@osu.edu (P.K. Dutta).

http://dx.doi.org/10.1016/j.micromeso.2016.04.042
1387-1811/© 2016 Elsevier Inc. All rights reserved.

serve as membrane materials for continuous CO_2 separation [15]. Pore size modification of siliceous CHA by chemical vapor deposition increases selectivity of CO_2/N_2 separation [16]. A molecular basis for CO_2 adsorption by CHA based on specific interactions with cations has been noted [17]. SAPO-34 which has the CHA structure showed selectivity of 36, 16 and 7.5 for CO_2/CH_4, CO_2/N_2 and H_2/CH_4 separation, respectively [18]. SSZ-13 also has the CHA structure (with Si/Al of 14), and exhibited selectivity of 12, 8.2 and 5.7 at 298 K for CO_2/CH_4, H_2/CH_4 and $H_2/n\text{-}C_4H_{10}$ separations, respectively [19]. High silica SSZ-13 was also shown to have excellent CO_2 adsorption capacity, particularly the Li^+ and Na^+ exchanged samples [20]. Other applications of chabazite include desiccants and for removal of radioactive contamination [21].

CO_2 is preferentially adsorbed on zeolites over N_2 since it has stronger intermolecular interactions with polar surfaces, the reason being the higher quadrupole moment and polarizability for CO_2 (-1.4×10^{-39} cm^2 and 29×10^{-25} cm^{-3}) as compared with N_2 (-4.7×10^{-40} cm^2 and 17.4×10^{-25} cm^{-3}) [22,23]. With CHA, molecular sieving would not work for CO_2 (kinetic diameter = 0.33 nm) separation from N_2 (kinetic diameter = 0.364 nm), since the CHA pore size (0.38 nm) is still larger than the size of N_2. However, cations that are present in the pore apertures of CHA can play a role in controlling the entry of molecule into the cages. Molecules, such as CO_2, can pay the energy price to displace the "door-keeping" cations (such as K^+) and thus gain admittance to the zeolite supercage, whereas molecules, such as N_2, are excluded ("molecular trapdoor" effect) [24].

There is limited literature involved in chabazite membrane preparation, with applications focused on pervaporation. Hasegawa et al. [25,26] prepared chabazite membranes in a synthesis gel containing strontium cation, which worked as a pseudo-template for crystal growth of the CHA-type zeolite. Li et al. [27] synthesized chabazite membrane in the presence of potassium cation. The seeds for secondary growth of these membranes was prepared by the conversion of micron-sized zeolite Y-type crystal [25–30], or from zeolite T [28]. Different substrates have been used for the growth of CHA membranes, such as mullite [27], porous $\alpha\text{-}Al_2O_3$ [25,29,30], and stainless steel [28].

An alternative to inorganic materials as supports are polymers. To the best of our knowledge, growing CHA membrane on polymer support and demonstrating its viability for CO_2/N_2 separation has not yet been reported. We have reported a rapid crystallization synthesis procedure of FAU membranes with potential for scale-up [31]. This procedure, abbreviated as DRHT (dehydration rehydration hydrothermal) involves dehydration of a reaction gel followed by re-addition of water back to the reaction medium after a period, and resulted in faster crystallization. Here, this procedure is extended to the CHA structure. It is well known that aluminous CHA zeolite can be grown from FAU by interzeolite conversion in the presence of KOH, and is our choice for synthesis of CHA in this study [32]. We also report on the synthesis of isolated chabazite nanoparticles, and used it for seeding the polymer membrane. Structural characteristics of the chabazite/polymer composite membrane were evaluated. Transport properties of these membranes for CO_2/N_2 separation are reported.

2. Experimental

2.1. Synthesis of zeolite Y nanoparticles

40 nm zeolite Y was prepared from the molar composition 0.048 Na_2O; 1 Al_2O_3; 4.35 SiO_2; 249 H_2O; 2.40 $(TMA)_2O(2OH)$; 1.2 $(TMA)_2O(2Br)$ based on a reported procedure [33]. First, aqueous 30 wt% colloidal silica (Ludox SM-30, Sigma-Aldrich) was ion exchanged with acidic cation exchange resin (Dowex Marathon C hydrogen form) until pH = 8, and then mixed with appropriate amounts of 25 wt% aqueous tetramethylammonium hydroxide solution (TMAOH, SACHEM) as solution A. Solution B containing distilled water, 25 wt% aqueous tetramethylammonium hydroxide solution, and aluminum isopropoxide (97 wt%, Sigma-Aldrich), was stirred vigorously at 70 °C until the solution became clear. TMABr (98 wt%, Sigma-Aldrich) was then added to the solution B and stirred until completely dissolved. Solution A was then mixed with solution B, and the bottle was sealed tightly and aged for 3 days at room temperature with vigorous stirring. The aged gel was heated with stirring in an oil bath at 100 °C for 4 days. The product was dialyzed in distilled water and washed by centrifugation until pH neutral; then decanting, and redispersion in distilled water with ultrasonication.

2.2. Synthesis of chabazite nanoparticles

The CHA seeds for secondary growth was prepared by the interzeolitic conversion of zeolite Y. 40 nm zeolite Y was dispersed in 100 mL 0.1 mol/L acetic acid at room temperature with stirring overnight to form proton-exchanged zeolite Y (H-Y). The ion-exchanged sample was washed by centrifugation five times in DI water. Potassium chabazite was synthesized following a reported procedure [34]. Typically, 1 g H-Y was added to 39.64 g DI water and 5.36 mL 45 wt% KOH solution. The molar composition of the prepared gel was 0.048 Na_2O; 8.4 K_2O; 1 Al_2O_3; 4.35 SiO_2; 593.6 H_2O. The mixture was aged 24 h at room temperature and heated under reflux at boiling for 3 days. The product was centrifuged, washed by DI water, and ultrasonicated.

2.3. DRHT method for rapid synthesis of CHA powders

CHA-type zeolite gel was prepared by the inter-zeolitic conversion method from FAU. To form a reaction gel of composition of 0.17 Na_2O: 2.0 K_2O: Al_2O_3: 5.18 SiO_2: 224 H_2O, 7.57 g of zeolite HY powder (CBV 400, Zeolyst) was added to 8.11 mL KOH 45% solution and 60.0 g distilled water. The synthesis was carried out by the DRHT method. The aged gel was transferred to a round bottom flask connected to a graduated pressure equalizing addition funnel topped with a condenser (Fig. 1S). The initial gel was heated under reflux for 1 h (temperature of reflux was 100 °C). Then over a period of 30 min, about 30 mL water was removed from the reaction system under reflux by condensation in the addition funnel (about half the volume of water in the flask), and the reflux continued. After 2 h in this concentrated state, the collected water was then re-added back dropwise from the funnel to the concentrated gel over a period of 30 min under reflux, and then the reaction continued under reflux. Samples were removed at various times during the synthesis process. Once removed, samples were immediately cooled in an ice bath for 1 h followed by 30 min of centrifugation at 2500 rpm. The pellets were lyophilized and stored under vacuum (50 mTorr) until analysis.

2.4. Chabazite/polymer composite membrane synthesis

Polyethersulfone (PES) 300 kDa supports were purchased from MILLIPORE Biomax. Nanocrystalline zeolite seed layer on PES support was prepared by vacuum dip-coating. The seeded support was placed in a sample holder and introduced into the DRHT reactor after dehydration (i.e. after removal of 30 mL water and prior to the 2 h reflux). The composition used was 0.17 Na_2O: 2.0 K_2O: Al_2O_3: 5.18 SiO_2: 224 H_2O. Then water was added back and the synthesis was continued under reflux. After washing by distilled water and drying at room temperature in air, the as-synthesized membrane was spin coated with 5 wt% polydimethylsiloxane (PDMS)

monomer solution. PDMS monomer solution was prepared by adding DEHESIVE 944, CROSSLINKER V 24 and CATALYST OL (Wacker Silicones, Inc) in the ratio of 100:1:0.5 to heptane, shaken vigorously and immediately applied for spin coating. DEHESIVE 944 is a solvent-based addition crosslinkable silicone. CROSSLINKER V 24 is a solvent free polysiloxane containing a high percentage of reactive Si-H groups. CATALYST OL is a highly-active platinum complex used for the thermal curing of addition-crosslinking, solvent-based and solventless silicones. For spin coating of PDMS onto a zeolite membrane, the membrane was first taped on the flat plate of the spin coater and PDMS monomer dispersion was added to cover the whole membrane. Spinning process consisted of 2000 rpm spin for 5 s and then 4000 rpm spin for 1 min. After spin coating, the membranes were kept at room temperature overnight for crosslinking of the PDMS.

2.5. Characterization

The phase and crystallinity of the zeolites were analyzed by a Bruker D8 Advance X-ray diffractometer. The surface morphology was investigated by a FEI Nova 400 NanoSEM scanning electron microscope. Transmission electron micrographs were collected using a FEI Tecnai F20 S/TEM. The particle size was measured by Dynamic Light Scattering (DLS) on a Malvern Zetasizer. Raman spectra were recorded using a Renishaw – Smiths Detection Combined Raman – IR Microprobe with the 514 nm line of an Ar^+ laser. The larger size powders CHA made by the hydrothermal and DRHT method were analyzed by a Bruker Avance III HD 400 MHz NMR spectrometer using 7 mm MAS probe. The sample was spun at 6 kHz and MAS spectrum acquired using Hahn Echo pulse sequence,

$$(\text{recovery period}) - \frac{\pi}{2} - \tau - \pi - \tau - (\text{acquisition}) \rightarrow$$

with the following parameters. recovery period = 300 s, $\pi/2$ and π timing set to 5.5 μs and 11 μs, respectively, and $\tau = 6\ \mu s$. The dwell time was set to 12.6 μs with 2048 acquisition points adding to a total of 5.16 ms of acquisition time. The number of scans for CHA was 376 and DRHT CHA powder was 550. Nano CHA was analyzed with a Bruker 800 MHz spectrometer using 2.5 mm MAS probe. The sample was spun at 20 kHz and the MAS spectrum was acquired using Hahn echo sequence with proton decoupling (>100 kHz). The $\pi/2$ time was set to 6.2 μs (Table 1S details the calculations for obtaining the Si/Al ratio).

A gas separation setup was constructed for CO_2/N_2 separation. The synthesized composite membrane was loaded into a stainless steel rectangular permeation cell inside a temperature-controlled oven with an effective membrane area of 3.4 cm^2. Feed gas and sweep gas compositions were controlled with a flow box and mass flow controllers from SIERRA Instruments Inc. A countercurrent flow configuration with a dry feed gas flow rate of 50 sccm and a dry sweep gas flow rate of 50 sccm was applied to offer the maximum driving force across the membrane. The binary gas mixture containing 20% CO_2 and 80% N_2 was used as the feed gas, while helium was used as the sweep gas. The testing pressures were 20 psig for the feed side and 20 psig for the sweep side, respectively. The outlet gas compositions of both retentate and permeate streams were analyzed by a SRI 310C gas chromatograph equipped with a Hysep D column and TCD detector. From the GC analysis, CO_2 permeance and CO_2/N_2 selectivity were calculated to characterize the membrane transport performance.

Permeance was calculated from the following equation:

$$\text{Permeance} = \frac{\text{mole of gas transferred per unit time}}{(\text{membrane area})(\text{partial pressure difference})}$$

and selectivity of CO_2 to N_2 was defined by the ratio of permeances.

The unit of permeance used is the gas permeation unit (GPU), 1 GPU = 3.35×10^{-10} mol/(m^2 s Pa).

3. Results and discussion

The following sections present the results of CHA zeolite/polymer composite membranes for CO_2/N_2 separation, including synthesis of nanocrystalline CHA zeolite seeds, rapid synthesis of CHA powders, synthesis of CHA membranes using the rapid method, and transport properties of CHA membranes.

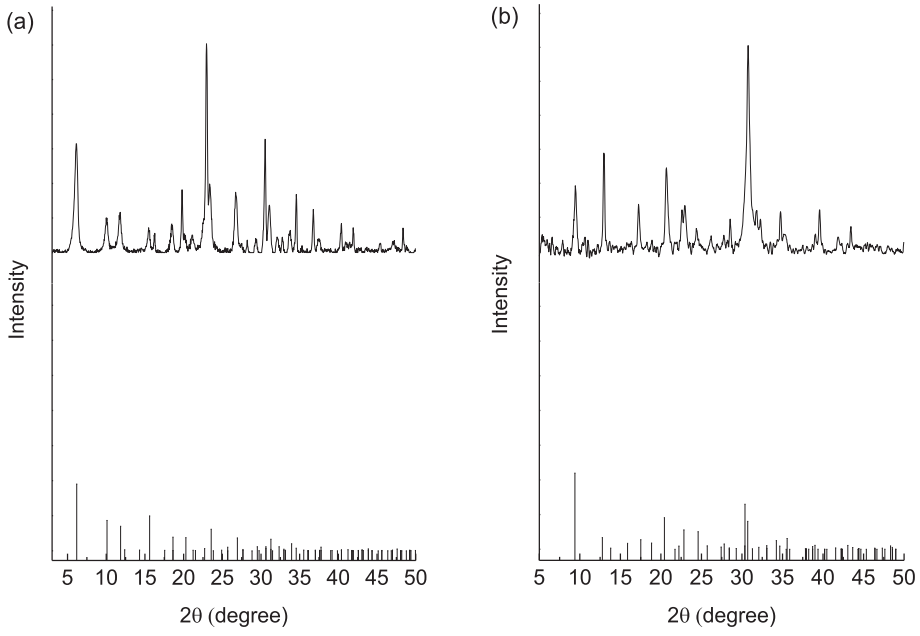

Fig. 1. (a) XRD patterns of zeolite Y nanoparticles and simulated FAU framework; (b) XRD patterns of chabazite nanoparticles and simulated CHA framework.

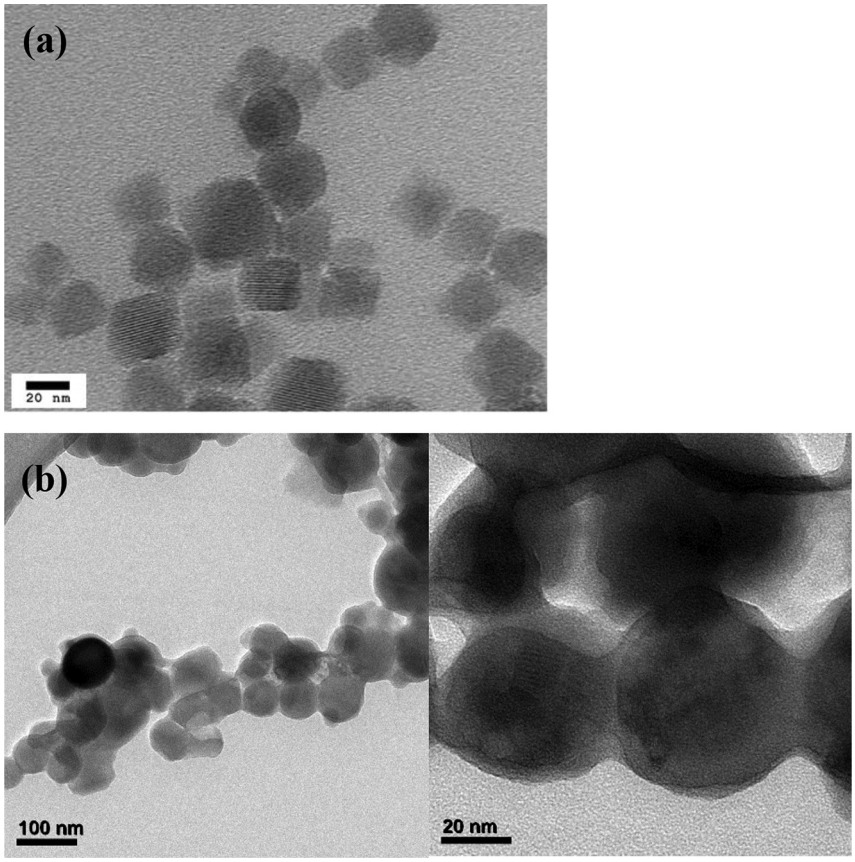

Fig. 2. (a) TEM image of zeolite Y nanoparticles; (b) TEM image of chabazite nanoparticles.

3.1. Synthesis of nanocrystalline CHA zeolite

Interzeolite conversion of FAU type zeolite to various different types of zeolites is well known, including formation of BEA [35], RUT [36], LEV [37] and CHA [38], often in the presence of structure-directing agents. The crystallization rate is enhanced and it is proposed that decomposition/dissolution of the starting zeolite generates locally ordered aluminosilicate species that assemble and evolve into another type of zeolite. The transformation of more open FAU-type zeolite with a framework density (FD) of 13.3 T/1000 $Å^3$ to the more condensed CHA with a FD of 15.1 T/1000 $Å^3$ zeolite is also thermodynamically favored.

The interzeolite conversion of FAU nanocrystals to CHA was examined. The XRD pattern of FAU crystals showed the presence of pure-phase faujasite (Fig. 1a). Based on the morphology shown in the TEM image (Fig. 2a), the size of the FAU nanoparticles were between 20 and 30 nm, and showed well-formed nanocrystals with the lattice spacing of 14 Å attributed to the (111) planes of the FAU structure. The particle size distribution obtained from DLS analysis is shown in Fig. 2S, indicating the suspension contains particles with a distribution ranging from 15 to 90 nm. The average particle size is 38 nm, which is in a good agreement with the TEM observations.

Using these isolated FAU nanoparticles, nano-sized CHA crystals were prepared. XRD pattern shown in Fig. 1b is consistent with the CHA-type structure. Fig. 2b shows the TEM image of the CHA nanoparticles with crystal size of 50–100 nm. DLS analysis shows the size distribution from 40 to 180 nm with an average particle size of 90 nm (Fig. 2S). The particle size distribution in the nanosize range, and the translucent suspension indicates that isolated CHA nanoparticles are being produced.

Fig. 3a shows the ^{29}Si solid-state NMR of the CHA nanocrystals, and the Si/Al ratio is calculated to be 1.76 ± 0.05 (Table 1S has the details of the NMR calculation). Fig. 3b is the Raman spectrum of the CHA nanocrystals with bands at 323, 460 and 475 cm^{-1} characteristic of natural CHA crystals, in particular the splitting of the T-O-T bending mode at ~470 cm^{-1} [39,40]. There are a few reports of synthesis of nanosize CHA crystals. Pure CHA-type aluminosilicate zeolite with high crystallinity has been synthesized from an amorphous aluminosilicate gel with the addition of sodium-type Al-containing SSZ-13 ([Al]-SSZ-13) as seed crystals, and resulted in the formation of agglomerates of 70–150 nm roundish cubic crystals [41]. The CHA crystals prepared by interzeolite conversion of 100 nm zeolite T displayed a 2–4 μm walnut shape composite with hundreds of sub-micrometer crystals [28]. Previous studies of smallest isolated CHA nano crystals were in ~280 nm size range [42]. These reported CHA seed crystals are too large to be deposited into the pores of the polymer substrate for seeding purposes.

3.2. Speeding up synthesis of chabazite powders by the DRHT process

The interzeolite conversion of micron-sized H-FAU to CHA was studied with both conventional and the DRHT process. Samples were collected at various times during the synthesis process. Fig. 4a shows the XRD peaks for the conventional hydrothermal synthesis

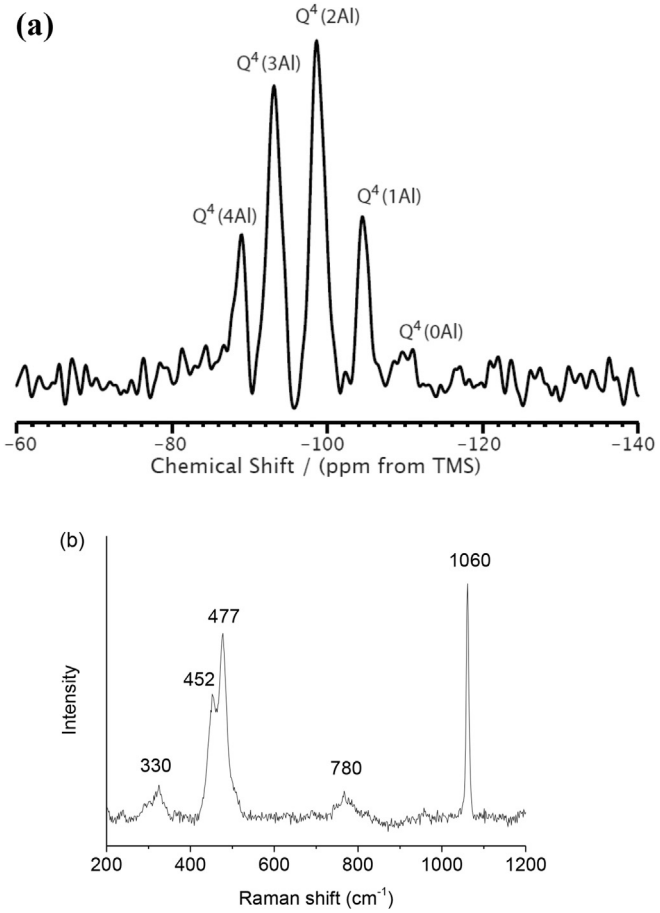

Fig. 3. (a) ^{29}Si MAS NMR spectra of CHA nanoparticles, a 100 Hz (FWHM) Gaussian apodization was applied prior to Fourier transformation; (b) Raman spectrum of CHA nanoparticles.

with CHA peaks appearing at 24 h with completion of the process between 96 and 118 h.

The synthesis was repeated with the DRHT process, which involved putting the aged gel through three stages in a reflux apparatus (shown in Fig. 1S). During stage I, half of the water was removed during reflux over a period of 30 min, and in stage II, the concentrated gel was kept in reflux for 2 h, and in stage III, water was added back during the course of 30 min during reflux. The heating process was continued. The XRD patterns of samples isolated at different times is shown in Fig. 4b. Within 8 h, a diffraction pattern showing the (100) peak of CHA at $2\theta = 9.4$ is evident. The XRD pattern continues to develop with time, and the peaks increase in intensity until reaching completion around 48 h.

The comparison of the crystallization process of CHA powders between the DRHT and the conventional synthesis is better demonstrated in Fig. 4c by plotting the relative peak intensity of the (100) peak at $2\theta = 9.4$ as a function of time. The crystallization of CHA is speeded up considerably by the DRHT process. Figs. 3S–5S compares the structural characteristics of the CHA powders obtained by the conventional and DRHT method. The morphologies obtained by SEM are similar with particle sizes of 1–2 μm, made up of aggregates of sub-micron crystals (Fig. 3S). The Raman spectra are also similar with all of the characteristic peaks for CHA (Fig. 4S). The ^{29} Si solid-state NMR of the CHA led to Si/Al ratio of 1.93 ± 0.08 for both the conventional and DRHT method (Fig. 5S), comparable to Si/Al of 2.15 reported in the literature [34].

3.3. Synthesis of chabazite membrane on polymer support by the DRHT process

The rapid DRHT synthesis procedure was adapted for CHA membrane formation. Nano CHA zeolite was coated on the PES support by applying vacuum on the back side of the PES support. The concentrated gel in the reactor formed after 2 h of reflux and removal of 30 mL water was used as the starting reactant, and the seeded support was introduced into this concentrated gel by interrupting the reaction. The reaction was continued by dripping the water back under reflux conditions for 30 min and then heated for a total of 44 h, after which the sample was withdrawn, washed by distilled water and dried in air. XRD of as synthesized membrane showed no evidence of a CHA zeolite membrane, though the powder collected from the reactor was well formed CHA (Fig. 6S).

Then, the DRHT procedure was repeated with nano-FAU seeds. The 40 nm zeolite Y nanoparticles were ion-exchanged with acetic acid to make H-form zeolite Y, which were loaded into the PES and the DRHT process carried out. This strategy involves the H-Y seed conversion in the pores of the PES to CHA, as well as micron-sized H-Y in the reaction gel to grow the CHA membrane on top of the PES membrane.

Fig. 5a shows the SEM of the bare PES support, with pores of 50–200 nm. The SEM of the nano H-Y seed coated PES (top view) is shown in Fig. 5b. SEM of a side view of the seeded layer is shown in Fig. 7S. The seed layer is ~3 to 4 μm thick, and a fraction of the nanozeolite seed crystals penetrate into the PES layer. The SEM in Fig. 5c after the DRHT process shows a layer on top of the PES involving intergrown particles. From the cross-section SEM images in Fig. 5d, there exists a dense skin layer on the PES support with an apparent thickness of 4 μm. Another angular view of the CHA membrane is shown in Fig. 8S.

Fig. 6a shows that the XRD of the membrane has the characteristics peaks of chabazite. Fig. 6b shows the Raman spectrum with the characteristic CHA peak at 470 cm^{-1}. The PES was dissolved by N-methylpyrrolidone, leaving behind a powder-like white film. Fig. 6c is a top-view SEM image of the film, which on a closer inspection is a collection of crystals with the same geometrical features as the original zeolite membrane. There are no cracks in this film. A network of submicron zeolite crystals has grown through the entire PES network that has three-dimensional interconnectivity with the zeolite layer on top of the PES. The growth within the porous support is important for CHA membrane stability, a feature we have noted before with FAU membranes [43]. This growth within the PES layer is initiated with the 40 nm nano HY seeds that penetrate within the PES. We speculate that this is the reason why the seeding with the 90 nm CHA seeds did not end up in forming the CHA membrane, though the reaction did form CHA powder. The size of CHA seed (90 nm) reduces the entry into the PES pores, leading to lack of crystal growth within the PES pores, a feature necessary for anchoring the membrane on top of the polymer support. Using HY as starting reactant, a previous study has noted that even after 5 days of hydrothermal treatment at ~100 °C, suitable defect-free CHA membranes on inorganic supports were not formed [27].

Considering that the PES membrane is in a highly basic solution at 100 °C for 44 h, we tested the integrity of the PES under these conditions. Fig. 9S shows the electron micrograph, XRD patterns and Raman spectra of PES subjected to 44 h of hydrothermal

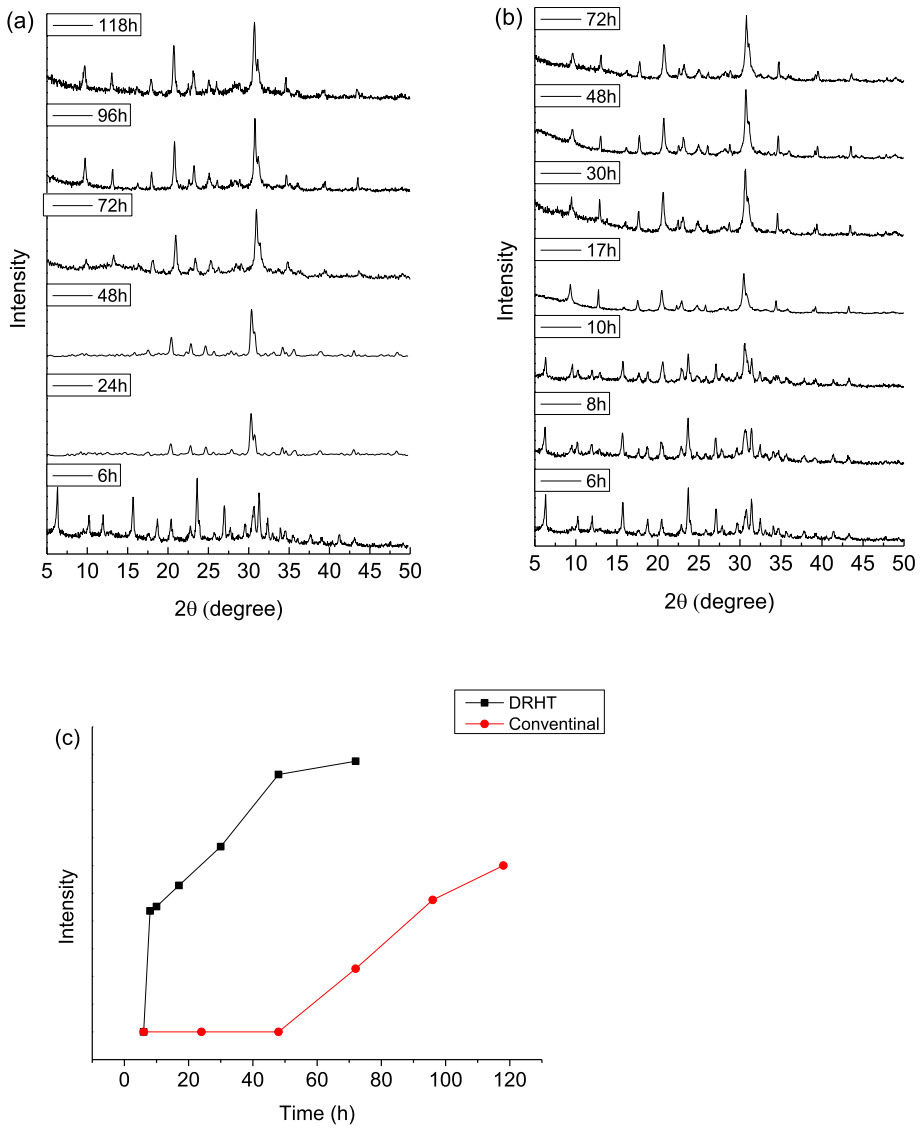

Fig. 4. (a) XRD patterns of samples recovered at intermediate stages during interzeolite conversion of FAU to CHA using the conventional hydrothermal synthesis process; (b) XRD patterns of samples recovered at intermediate stages during interzeolite conversion of FAU to CHA using the DRHT process; (c) Comparison of the crystallization process between the DRHT method and the conventional hydrothermal synthesis for FAU to CHA conversion (plot of intensity of the $2\theta = 9.4$ peak of CHA).

treatment. The morphological and spectroscopic properties remain unchanged with hydrothermal treatment.

3.4. Transport properties of CHA zeolite/polymer composite membranes

The transport properties of three types of membranes were examined. In each case, the PES supports were coated with PDMS. PDMS is commonly used as sealing material to seal defects on porous polymeric materials, as well as zeolite membranes [44,45]. PDMS (5 wt%) was coated on the bare PES support, on the H-Y (nanoseeds) coated PES and on the CHA/PES membrane that was formed by the method described above. The transport data related to CO_2/N_2 separation were carried out at 25, 50 and 75 °C. All transport data are reported in Table 1 (standard deviations based on three membranes). Without PDMS coating, there is no selectivity of CO_2 over N_2 (CO_2 permeance = ~5000 GPU, CO_2/N_2 selectivity = 1), indicating that there are intercrystalline defects through which the gas molecules can pass. The strategy for using PDMS was that the monomers would penetrate into the intercrystalline defects and then upon polymerization, the defects would be sealed. With the PDMS/PES, at room temperature, the CO_2/N_2 selectivity was around 4 with a CO_2 permeance of 3820 GPU. With the PDMS/HY seed coated PES the CO_2/N_2 selectivity was around 10 with a CO_2 permeance of 1748 GPU. For the PDMS on the CHA/PES membrane, the CO_2/N_2 selectivity was around 19 with a CO_2 permeance of 1243 GPU. The permeance in all cases increased with temperature, and the CO_2/N_2 selectivity decreased. It is clear that with formation of the CHA membrane there is improvement in the CO_2/N_2 selectivity. There are many instances of mixed matrix membranes reported in the literature [46], and the PDMS/HY-seeded membrane resembles best the mixed matrix membrane. The improvement of the transport property with the CHA/PES membrane over the seeded membrane indicates that the growth of CHA crystals within and on top of the PES is critical to the improved separation performance. We conclude that separation occurring with the CHA/PES membrane is because the CO_2/N_2 separation is occurring within the CHA pores.

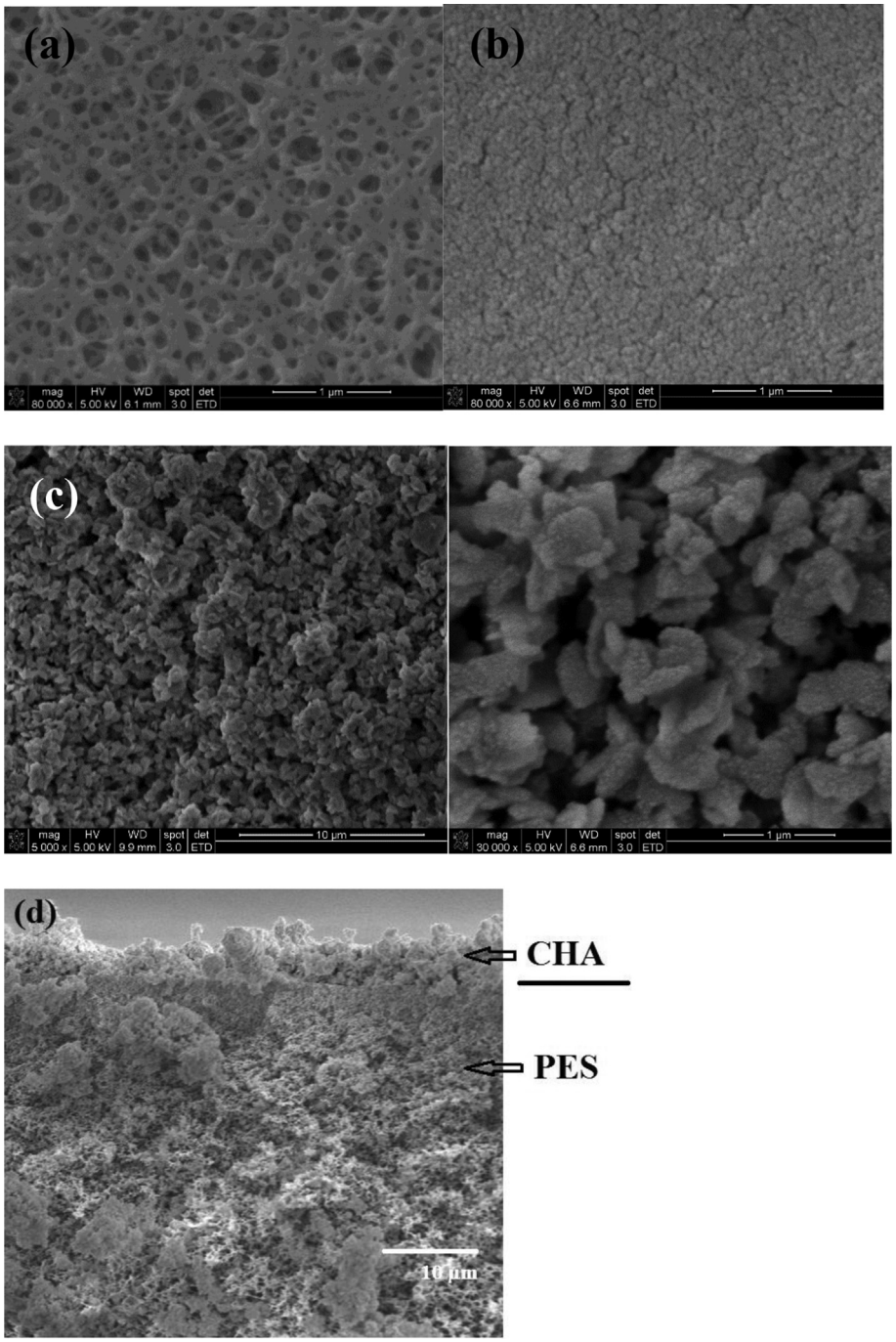

Fig. 5. (a) SEM image of PES support; (b) SEM image of nanoHY seed coated on PES support; (c) SEM of CHA membrane/PES formed via the DRHT process after 44 h growth; (d) Cross section SEM image of CHA membrane/PES formed via the DRHT process after 44 h growth.

4. Conclusions

CHA nanocrystals were synthesized by interzeolite conversion of H-form of zeolite Y nanocrystals. The DRHT (dehydration rehydration hydrothermal) method led to rapid synthesis of CHA powders, with a 2-fold increase in the rate of crystal growth, as compared to conventional hydrothermal process. The initial dehydration leads to extensive nucleation, maintaining the concentrated state enhances the nucleation, and controlled re-addition of water leads to an overall increase in the rate of crystal growth. Chabazite membranes on PES supports were prepared by the DRHT method using nano FAU seeds by a secondary growth method using interzeolite conversion of FAU. CHA growth within the porous polymer layer was necessary for anchoring the zeolite membrane on top of the PES support. Transport properties of PDMS coated PES, PDMS coated HY seeded PES and PDMS coated CHA membrane on PES were studied. The CO_2/N_2 selectivity at room temperature was found to be 4, 10.4 and 18.6 for PDMS/PES, PDMS/HY-seeded PES and PDMA/CHA/PES, indicating that the CHA membranes were exhibiting selective separation of CO_2.

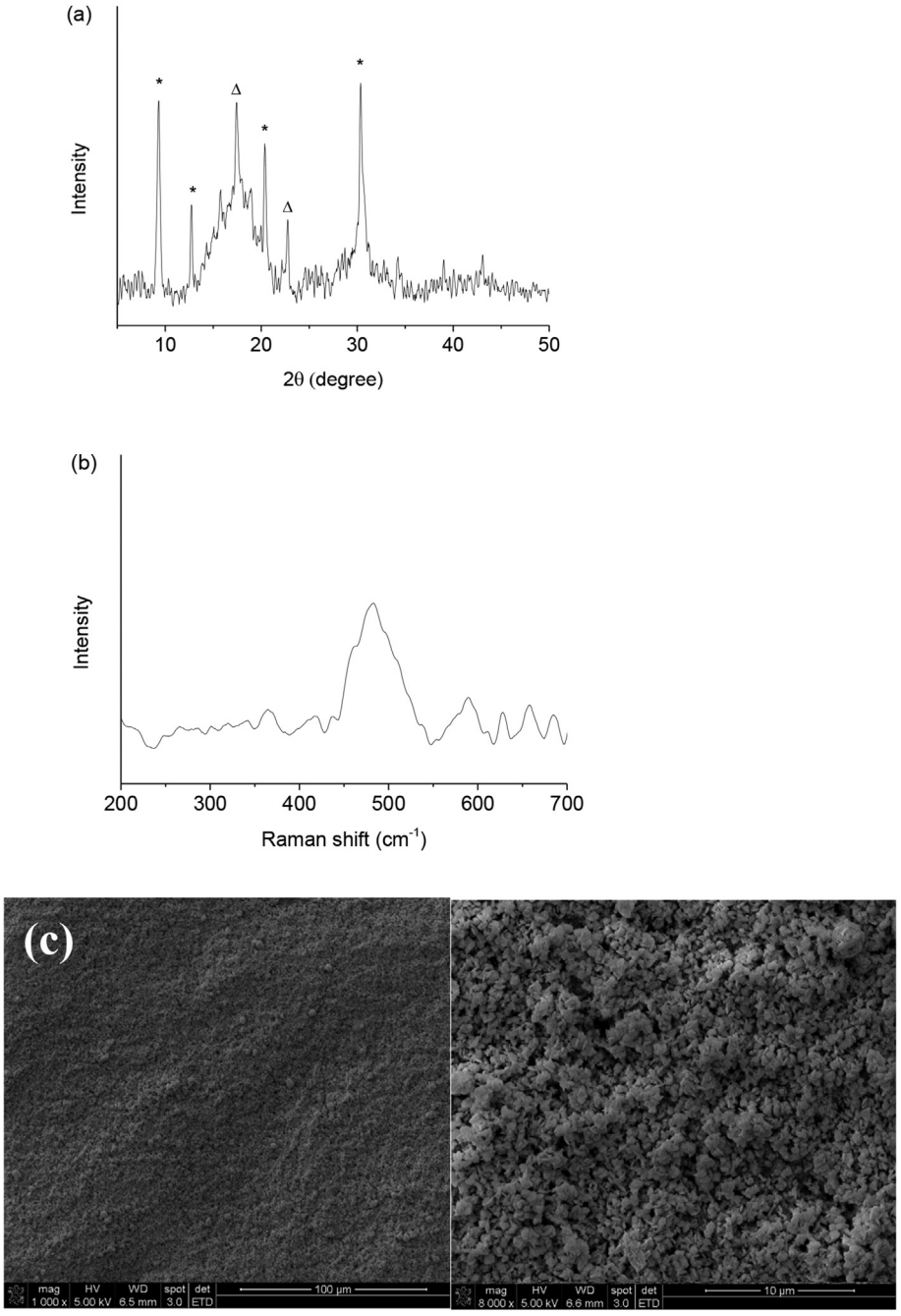

Fig. 6. (a) XRD of CHA membrane/PES formed via the DRHT process after 44 h growth (CHA peaks are indicated with asterisks (*), PES support peaks are indicated with triangles (Δ)); (b) Raman spectra of CHA membrane/PES formed via the DRHT process after 44 h growth; (c) Top-view SEM image of CHA/PES membrane after dissolution of PES with N-methyl pyrrolidone. Left: low magnification image, right: high magnification image.

Table 1
Transport properties of 5 wt% PDMS coated on various PES membranes using 20% CO_2/N_2 (three samples were used for each set of data).

	25 °C		50 °C		75 °C	
	CO_2 permeance (GPU)	CO_2/N_2 selectivity	CO_2 permeance (GPU)	CO_2/N_2 selectivity	CO_2 permeance (GPU)	CO_2/N_2 selectivity
PDMS/PES	3821 ± 14	4.08 ± 0.04	4058 ± 4.0	3.72 ± 0.14	4077 ± 13	3.31 ± 0.12
PDMS/seed/PES	1748 ± 10	10.4 ± 0.04	1786 ± 7.0	9.5 ± 0.12	1803 ± 15	8.2 ± 0.15
PDMS/CHA/PES membrane	1243 ± 2.5	18.63 ± 0.03	1269 ± 11	17.34 ± 0.09	1290 ± 18	16.34 ± 0.14

Acknowledgement

This work is funded by The U.S. Department of Energy under Award Number DE-FE0007632. However, any opinions, findings, conclusions, or recommendations expressed herein are those of the author(s) and do not necessarily reflect the views of the DOE. We thank Dr. Tanya Whitmer for recording the NMR spectra.

Appendix A. Supplementary data

Supplementary data related to this article can be found at http://dx.doi.org/10.1016/j.micromeso.2016.04.042.

References

[1] D.M. D'Alessandro, B. Smit, J.R. Long, Carbon dioxide capture: prospects for new materials, Angew. Chem. Int. Ed. 49 (2010) 6058–6082.
[2] N. MacDowell, N. Florin, A. Buchard, J. Hallett, A. Galindo, G. Jackson, C.S. Adjiman, C.K. Williams, N. Shah, P. Fennell, An overview of CO_2 capture technologies, Energy Environ. Sci. 3 (2010) 1645–1669.
[3] J.D. Figueroa, T. Fout, S. Plasynski, H. McIlvried, R.D. Srivastava, Advances in CO_2 capture technology—the US department of Energy's carbon sequestration program, Int. J. Greenh. Gas control. 2 (2008) 9–20.
[4] T.C. Merkel, H. Lin, X. Wei, R. Baker, Power plant post-combustion carbon dioxide capture: an opportunity for membranes, J. Membr. Sci. 359 (2010) 126–139.
[5] N. Rangnekar, N. Mittal, B. Elyassi, J. Caro, M. Tsapatsis, Zeolite membranes–a review and comparison with MOFs, Chem. Soc. Rev. 44 (2015) 7128–7154.
[6] J. Caro, M. Noack, P. Kölsch, R. Schäfer, Zeolite membranes–state of their development and perspective, Microporous mesoporous Mater. 38 (2000) 3–24.
[7] J. Gascon, F. Kapteijn, B. Zornoza, V. Sebastián, C. Casado, J. Coronas, Practical approach to zeolitic membranes and coatings: state of the art, opportunities, barriers, and future perspectives, Chem. Mater. 24 (2012) 2829–2844.
[8] Y. Morigami, M. Kondo, J. Abe, H. Kita, K. Okamoto, The first large-scale pervaporation plant using tubular-type module with zeolite NaA membrane, Sep. Purif. Technol. 25 (2001) 251–260.
[9] E. McLeary, J. Jansen, F. Kapteijn, Zeolite based films, membranes and membrane reactors: progress and prospects, Microporous Mesoporous Mater. 90 (2006) 198–220.
[10] K. Kusakabe, T. Kuroda, K. Uchino, Y. Hasegawa, S. Morooka, Gas permeation properties of ion-exchanged faujasite-type zeolite membranes, AIChE J. 45 (1999) 1220–1226.
[11] J.C. White, P.K. Dutta, K. Shqau, H. Verweij, Synthesis of ultrathin zeolite Y membranes and their application for separation of carbon dioxide and nitrogen gases, Langmuir 26 (2010) 10287–10293.
[12] O. Yakubovich, W. Massa, P. Gavrilenko, I. Pekov, Crystal structure of chabazite K, Crystallogr. Rep. 50 (2005) 544–553.
[13] T. Inui, Y. Okugawa, M. Yasuda, Relationship between properties of various zeolites and their carbon dioxide adsorption behaviors in pressure swing adsorption operation, Ind. Eng. Chem. Res. 27 (1988) 1103–1109.
[14] J. Zhang, R. Singh, P.A. Webley, Alkali and alkaline-earth cation exchanged chabazite zeolites for adsorption based CO_2 capture, Microporous Mesoporous Mater. 111 (2008) 478–487.
[15] R. Krishna, J.M. van Baten, In silico screening of zeolite membranes for CO_2 capture, J. Membr. Sci. 360 (2010) 323–333.
[16] E. Kim, T. Lee, H. Kim, W.-J. Jung, D.-Y. Han, H. Baik, N. Choi, J. Choi, Chemical vapor deposition on chabazite (CHA) zeolite membranes for effective post-combustion CO_2 capture, Environ. Sci. Technol. 48 (2014) 14828–14836.
[17] T.D. Pham, M.R. Hudson, C.M. Brown, R.F. Lobo, Molecular basis for the high CO_2 adsorption capacity of chabazite zeolites, ChemSusChem 7 (2014) 3031–3038.
[18] J.C. Poshusta, V.A. Tuan, E.A. Pape, R.D. Noble, J.L. Falconer, Separation of light gas mixtures using SAPO-34 membranes, AIChE J. 46 (2000) 779–789.
[19] H. Kalipcilar, T.C. Bowen, R.D. Noble, J.L. Falconer, Synthesis and separation performance of SSZ-13 zeolite membranes on tubular supports, Chem. Mater. 14 (2002) 3458–3464.
[20] T.D. Pham, Q. Liu, R.F. Lobo, Carbon dioxide and nitrogen adsorption on cation-exchanged SSZ-13 zeolites, Langmuir 29 (2012) 832–839.
[21] F.A. Mumpton, La roca magica: uses of natural zeolites in agriculture and industry, Proc. Natl. Acad. Sci. 96 (1999) 3463–3470.
[22] K. Sumida, D.L. Rogow, J.A. Mason, T.M. McDonald, E.D. Bloch, Z.R. Herm, T.-H. Bae, J.R. Long, Carbon dioxide capture in metal–organic frameworks, Chem. Rev. 112 (2011) 724–781.
[23] C. Graham, D.A. Imrie, R.E. Raab, Measurement of the electric quadrupole moments of CO_2, CO, N_2, Cl_2 and BF_3, Mol. Phys. 93 (1998) 49–56.
[24] J. Shang, G. Li, R. Singh, P. Xiao, J.Z. Liu, P.A. Webley, Potassium chabazite: a potential nanocontainer for gas encapsulation, J. Phys. Chem. C 114 (2010) 22025–22031.
[25] Y. Hasegawa, H. Hotta, K. Sato, T. Nagase, F. Mizukami, Preparation of novel chabazite (CHA)-type zeolite layer on porous α-Al_2O_3 tube using template-free solution, J. Membr. Sci. 347 (2010) 193–196.
[26] Y. Hasegawa, C. Abe, M. Nishioka, K. Sato, T. Nagase, T. Hanaoka, Formation of high flux CHA-type zeolite membranes and their application to the dehydration of alcohol solutions, J. Membr. Sci. 364 (2010) 318–324.
[27] X. Li, H. Kita, H. Zhu, Z. Zhang, K. Tanaka, K.-i. Okamoto, Influence of the hydrothermal synthetic parameters on the pervaporative separation performances of CHA-type zeolite membranes, Microporous Mesoporous Mater. 143 (2011) 270–276.
[28] R. Zhou, Y. Li, B. Liu, N. Hu, X. Chen, H. Kita, Preparation of chabazite membranes by secondary growth using zeolite-T-directed chabazite seeds, Microporous Mesoporous Mater. 179 (2013) 128–135.
[29] S. Shirazian, S.N. Ashrafizadeh, Optimum conditions for the synthesis of CHA-type zeolite membranes applicable to the purification of natural gas, Ind. Eng. Chem. Res. 53 (2014) 12435–12444.
[30] A. Nouri, M. Jafari, M. Kazemimoghadam, T. Mohammadi, Potential separation of SF_6 from air using chabazite zeolite membranes, Chem. Eng. Technol. 37 (2014) 317–324.
[31] B. Wang, C. Sun, Y. Li, L. Zhao, W.W. Ho, P.K. Dutta, Rapid synthesis of faujasite/polyethersulfone composite membrane and application for CO_2/N_2 separation, Microporous Mesoporous Mater. 208 (2015) 72–82.
[32] R. Nedyalkova, C. Montreuil, C. Lambert, L. Olsson, Interzeolite conversion of FAU type zeolite into CHA and its application in NH_3-SCR, Top. Catal. 56 (2013) 550–557.
[33] B.A. Holmberg, H. Wang, J.M. Norbeck, Y. Yan, Controlling size and yield of zeolite Y nanocrystals using tetramethylammonium bromide, Microporous mesoporous Mater. 59 (2003) 13–28.
[34] H. Karge, H. Robson, Verified Syntheses of Zeolitic Materials, Elsevier, Amsterdam, 2001.
[35] H. Jon, K. Nakahata, B. Lu, Y. Oumi, T. Sano, Hydrothermal conversion of FAU into *BEA zeolites, Microporous mesoporous Mater. 96 (2006) 72–78.
[36] H. Jon, S. Takahashi, H. Sasaki, Y. Oumi, T. Sano, Hydrothermal conversion of FAU zeolite into RUT zeolite in TMAOH system, Microporous Mesoporous Mater. 113 (2008) 56–63.
[37] T. Inoue, M. Itakura, H. Jon, Y. Oumi, A. Takahashi, T. Fujitani, T. Sano, Synthesis of LEV zeolite by interzeolite conversion method and its catalytic performance in ethanol to olefins reaction, Microporous Mesoporous Mater. 122 (2009) 149–154.
[38] M. Itakura, T. Inoue, A. Takahashi, T. Fujitani, Y. Oumi, T. Sano, Synthesis of high-silica CHA zeolite from FAU zeolite in the presence of benzyltrimethylammonium hydroxide, Chem. Lett. 37 (2008) 908–909.
[39] D. Arkhipenko, G. Valueva, T. Moroz, Determination of the space group of chabazite, J. Struct. Chem. 36 (1995) 171–174.
[40] C.L. Angell, Raman spectroscopic investigation of zeolites and adsorbed molecules, J. Phys. Chem. 77 (1973) 222–227.
[41] H. Imai, N. Hayashida, T. Yokoi, T. Tatsumi, Direct crystallization of CHA-type zeolite from amorphous aluminosilicate gel by seed-assisted method in the absence of organic-structure-directing agents, Microporous Mesoporous Mater. 196 (2014) 341–348.
[42] Z. Bohström, B. Arstad, K.P. Lillerud, Preparation of high silica chabazite with controllable particle size, Microporous Mesoporous Mater. 195 (2014) 294–302.
[43] M. Severance, B. Wang, K. Ramasubramanian, L. Zhao, W.W. Ho, P.K. Dutta, Rapid crystallization of faujasitic zeolites: mechanism and application to zeolite membrane growth on polymer supports, Langmuir 30 (2014) 6929–6937.
[44] W. Chiu, I.-S. Park, K. Shqau, J. White, M. Schillo, W. Ho, P. Dutta, H. Verweij, Post-synthesis defect abatement of inorganic membranes for gas separation, J. Membr. Sci. 377 (2011) 182–190.
[45] J.M. Henis, M.K. Tripodi, A novel approach to gas separations using composite hollow fiber membranes,, Sep. Sci. Technol. 15 (1980) 1059–1068.
[46] G. Dong, H. Li, V. Chen, Challenges and opportunities for mixed-matrix membranes for gas separation, J. Mater. Chem. A 1 (2013) 4610–4630.